Ultrasound in Med. & Biol., Vol. 33, No. 8, pp. 1224–1235, 2007

0301-5629/07/$–see front matter

ELSEVIER

doi:10.1016/j.ultrasmedbio.2007.02.008

● *Original Contribution*

ASSESSMENT OF SEVERITY IN AORTIC STENOSIS—INCREMENTAL VALUE OF ENDOCARDIAL FUNCTION PARAMETERS COMPARED WITH STANDARD INDEXES

ANTONIO VITARELLI,* MIGUEL CORTES MORICHETTI,† YSABEL CONDE,* ESTER CIMINO,* SIMONA D'ORAZIO,* SIMONA STELLATO,* VIVIANA PADELLA, FIORELLA CARANCI, and DANIELA BATTAGLIA*

*"La Sapienza" University, Rome, Italy; and †European Hospital Georges Pompidou, Paris, France

(*Received* 15 *October* 2006; *revised* 1 *February* 2007; *in final form* 13 *February* 2007)

Abstract—Several studies have reported that patients (pts) with severe aortic stenosis and similar pressure gradients or even similar aortic valve areas may have quite different symptomatic status and clinical outcomes suggesting that other factors might have a significant impact on the pathophysiology of this disease. Our purpose was to assess the severity of subendocardial wall dysfunction in symptomatic and asymptomatic pts with aortic stenosis using tissue Doppler imaging (TDI), strain rate imaging (SRI) and cyclic variation of integrated backscatter (IB). We studied 68 pts with aortic valvar stenosis and 46 subjects with no signs of heart disease. SRI/IB indexes were calculated in the apical four chambers views at endocardial level. Early diastolic endocardial strain rate showed the best correlation with transvalvar pressure gradients and valve areas. Compared with controls, symptomatic pts showed a more marked decrease in endocardial strain, strain rate and cyclic variation of IB. Receiver operating characteristic (ROC) curves suggested that the thresholds offering an adequate compromise between sensitivity and specificity for the prediction of symptoms were ≥60 mm Hg for the pressure gradient, less than 0.60 cm^2/m^2 for aortic valve area, less than 20% for strain, less than 2.0 s^{-1} for strain rate and less than 3.0 dB for cyclic variation. The combination of pressure gradient, aortic valve area and SRI/IB parameters resulted in an improvement of the overall performance for predicting the symptomatic state. Thus, SRI/IB parameters have an incremental value in differentiating symptomatic and asymptomatic pts with aortic stenosis compared with conventional hemodynamic parameters. (E-mail: vitar@tiscali.it) © 2007 World Federation for Ultrasound in Medicine & Biology.

Key Words: **Echocardiography, Tissue Doppler imaging, Strain rate imaging, Strain imaging, Integrated backscatter, Subendocardial dysfunction, Aortic stenosis.**

INTRODUCTION

Several studies have reported that patients (pts) with severe aortic stenosis and similar pressure gradients or even similar aortic valve areas may have quite different symptomatic status and clinical outcomes (Bonow et al. 1998; Otto 2000; Garcia et al. 2000; Rosenhek et al. 2000). These observations suggest that factors other than pressure gradient or aortic valve area might have a significant impact on the clinical presentation of this disease.

Using a model that describes the relative contributions of the left ventricular wall thickening (Tongue et al. 2003), it has been seen that left ventricular longitudinal shortening may be selectively decreased in aortic stenosis, and hypothesized that this might be a marker of subendocardial ischemia as subendocardial myocardial fibers are oriented longitudinally. The introduction of Doppler measurement of myocardial wall velocities (tissue Doppler imaging, TDI) and the recently developed strain rate imaging (SRI) technique have made possible a more adequate assessment of global and regional systolic and diastolic myocardial function (Isaaz et al. 1989; Nagueh et al. 2001; Vinereanu et al. 2001; Vitarelli et al. 2001, 2003; Kowalski et al. 2001; Stoylen et al. 2001; Sutherland et al. 2004). Both in children (Kiraly et al. 2003; De Kort et al. 2006) and adults (Lindstrom and Wranne 1999) with severe aortic stenosis, alterations in tissue velocity versus time patterns have been reported both in systole and diastole.

Address correspondence to: Antonio Vitarelli, MD, "La Sapienza" University, Via Lima 35, 00198 Rome, Italy. E-mail: vitar@tiscali.it

Blunting of cyclic variation (CV) of integrated backscatter (IB) has also been described as a marker of myocardial ischemia and/or fibrosis both in experimental and human models (Di Bello et al. 2004). Cyclic variation is affected symmetrically with regional wall thickening and is less operator-dependent compared with wall motion analysis and, therefore, amenable to quantification.

No study has so far tested the relation between symptomatic status, subendocardial function and standard indices of severity in patients with aortic stenosis. The present study was undertaken to assess if tissue velocity, strain rate and integrated backscatter parameters can detect subendocardial myocardial dysfunction in those patients, to determine the association of these changes with the conventional grading of the severity of left ventricular outflow tract obstruction and to investigate the value of these indexes of subendocardial function in differentiating symptomatic and asymptomatic patients.

METHODS

Patients

We prospectively studied 68 pts aged 15 to 52 y with a clinical and echocardiographic diagnosis of aortic stenosis from January 2002 to May 2006. Fifty-five patients had bicuspid valves and 13 had tricuspid valves. Patients with moderate or severe coexisting aortic regurgitation or moderate or severe mitral valve regurgitation were excluded, as well as patients with known or suspected coexisting systemic hypertension or coronary artery disease. Patients with coarctation of the aorta or patients who presented with both valvar and subvalvar stenosis were also excluded to avoid additional factors affecting left ventricular pressure overload. On the basis of their symptomatic status, pts were distinguished in two groups: group 1 (37 pts), asymptomatic and group 2 (31 pts), symptomatic. An asymptomatic patient was defined as a patient who did not report any of the classic triad of symptoms: dyspnea, syncope or angina. Associated clinical conditions were previous infective endocarditis (three pts), and type 1 diabetes (one pt). Cardiac catheterization and coronary angiography were performed in 36 patients (older than 35 y) to rule out coronary artery disease. No patient underwent previous interventions before the echocardiographic studies. Twenty-seven patients had surgery (valvotomy or valve replacement) following echocardiographic studies either because of being symptomatic (23 patients) or because of trans-stenotic pressure gradients >70 mm Hg and/or valve areas <0.8 cm^2 (four patients). They were examined after 6 months to assess LV function. Forty-six age- and gender-matched subjects with no clinical and echocardiographic signs of heart disease were selected as normal controls. The investigation had the patient consent and approval of Internal Review Boards.

Echocardiography

All patients underwent a complete clinical examination as well as transthoracic and transesophageal echocardiography (Aplio Echocardiograph, Toshiba Co., Tokyo, Japan). Echocardiographic data were recorded with either a 2.5 or 3.5 MHz phased array transducer. Measurements of different cardiac chambers were made by transthoracic echocardiography according to established criteria (Schiller et al. 1989). Fractional shortening, ejection fraction by modified Simpson method, left ventricular mass index, end-systolic left ventricular meridional wall stress (ESS_m) and circumferential wall stress (ESS_c) were estimated (Borow et al. 1985; Devereux et al. 1986; Mirsky et al. 1988; Schiller 1989).

Peak early and late diastolic transmitral valve blood flow velocities, deceleration time, left ventricular isovolumic relaxation time, pulmonary venous Doppler recording were obtained from apical four chamber view using standard Doppler practices (Tenenbaum et al. 1996; Appleton et al. 1993).

Peak and mean transvalvular gradients were calculated by using the modified Bernoulli equation. Aortic valve area was determined by transthoracic echocardiography using the standard continuity equation (Oh et al. 1988; Rask et al. 1996; Donal 2005) and by transesophageal echocardiography using area planimetry (Hoffmann et al. 1993).

Tissue Doppler echocardiography

The general principles that underlie the TDI modalities have been previously described (McDicken et al. 1992). By using the transthoracic apical four-chamber views, the longitudinal ventricular wall motion velocities were assessed during the cardiac cycle. Velocities toward the transducer are color-coded red and velocities away from the transducer are coded blue. Two-dimensional (2D) tissue velocity images of the ventricular wall were obtained at $\geq$120 frames/s, which implies a temporal resolution of approximately 8 to 9 ms. By marking a region-of-interest on the 2D image with a sampling volume size of 3 $\times$ 3 pixels, velocities throughout the cardiac cycle for this area can be determined. The raw data were digitally stored and off-line analysis of the data sets was performed using dedicated software.

TDI wall velocities during systole, early relaxation and atrial systole were measured (Fig. 1) in endocardium (End) and epicardium (Epi) in both study groups in

apical four chambers views in the more basal part of the left ventricular free wall. Velocity and strain traces were processed from the same wall site in the same views (Fig. 1). From tissue Doppler data, strain rate (SR) can be estimated by calculating the velocity gradient (Kiraly et al. 2003; Vitarelli et al. 2003; Sutherland et al. 2004). SR equals the rate of regional myocardial deformation and is equivalent to the spatial gradient of velocity on the basis of the equation: $SR = (v - v[r + \Delta r])/\Delta r$ (Sutherland et al. 2004). Strain (ϵ, change in length per unit length) in each segment was defined as the degree of lengthening or compression (%) between two adjacent points in space. Peak systolic strain (ϵ) was determined (Fig. 1). Strain rate (SR) parameters were assessed during isovolumic contraction, systole, isovolumic relaxation, early diastole and late diastole in the same views. Peak negative SR during isovolumic contraction and peak positive SR during isovolumic relaxation were measured (Fig. 1). Isovolumic contraction was determined by the Q wave of the ECG and the closing of the mitral valve on 2D echocardiographic cine loop. Isovolumic relaxation was determined by the opening of the mitral valve of the cine loop. Peak negative SR during systole and peak positive SR during early and late diastole were measured (Fig. 1). The values of three measurements were averaged.

The auto tracking mode was used to keep the sampling volume over to same area of tissue during the contraction-relaxation cycle of the heart. In this way it was ensured that the dimensional changes within one region of the myocardial wall were measured and the partial volume effect of the left ventricular blood pool was avoided. The longitudinal strain in an endocardial position as opposed to an epicardial position was obtained. The spatial offset of 8 mm was selected as a compromise between acceptable signal-to-noise ratio and longitudinal spatial resolution.

TDI velocities during systole (S_a), early relaxation (E_a) and atrial systole (A_a) were also measured in the apical four chambers views at the lateral mitral annulus.

Integrated backscatter echocardiography

In the same wall sites, the magnitude of cyclic variation (CV) of integrated backscatter (IB) was determined (Fig. 1D) as the difference between the end-diastolic and end-systolic values in a cardiac cycle. End-diastole was defined as the point in the cardiac cycle corresponding to the onset of electrocardiographic Q wave. End-systole was defined as the time of apparent minimal left ventricular chamber size and occurred near the peak of the T wave. For each region-of-interest, a histogram of the echo gray level distribution was generated. The region-of-interest was always of the same size (3×3 mm) and placed in the same location of the wall. During analysis, the operator carefully adjusted the location of the region-of-interest in each frame to avoid inclusion of the specular reflections of the adjacent layer.

In assessing these endocardial echocardiographic indexes, the observers were blinded as to the clinical or the standard echo findings.

Statistics

Data are presented as mean value ±SD. Linear correlations and multiple correlation analysis were used for comparisons. Variables were compared between groups and differences were considered statistically significant when the p value was $<.05$. As the scores on the examination were continuous variables and normally distributed, parametric statistics were used for analysis. Nonparametric statistics were used for data that were not normally distributed. Receiver operating characteristic curves of echocardiographic indexes were tested with use of a maximum likelihood estimation approach for differences (Metz 1986). To test intraobserver variability, measurements of systolic and diastolic TDI were made at 50 sites in different patients on two different occasions. For interobserver variability, a second investigator randomly made measurements at the above different sites without knowledge of other echocardiographic parameters. The intraobserver and interobserver variabilities were determined (as the difference between the two sets of observations divided by the mean of the observations and expressed as a percentage).

RESULTS

Sixty-eight out of 71 initially evaluated patients were included in the study. Although great care was taken to ensure the quality of the data collected, three patients had to be excluded from analysis as the velocity/strain traces were defined to be noninterpretable. This was either due to low signal to noise ratio or to aliasing in the velocity data set, which had not been appreciated during acquisition. The intraobserver and interobserver reproducibility of wall velocities, wall peak systolic strain, strain rate and cyclic variation was shown to be acceptable. TDI parameters showed an intraobserver variability of 5.7% ± 3.4% (range 2.1 to 9.3, median 4.9) and interobserver variability of 6.8% ± 4.1% (range 2.4 to 11.6, median 6.6). SRI parameters had an intraobserver variability of 6.9% ± 4.3% (range 2.5 to 11.8, median 6.2) and interobserver variability of 8.1% ± 4.4% (range 3.4 to 12.8, median 8.7). For CV parameters, intraobserver variability was 4.9% ± 4.2% (range 0.6 to 9.4, median 4.1) and interobserver variability 5.5% ± 3.6% (range 1.7 to 9.9, median 6.2).

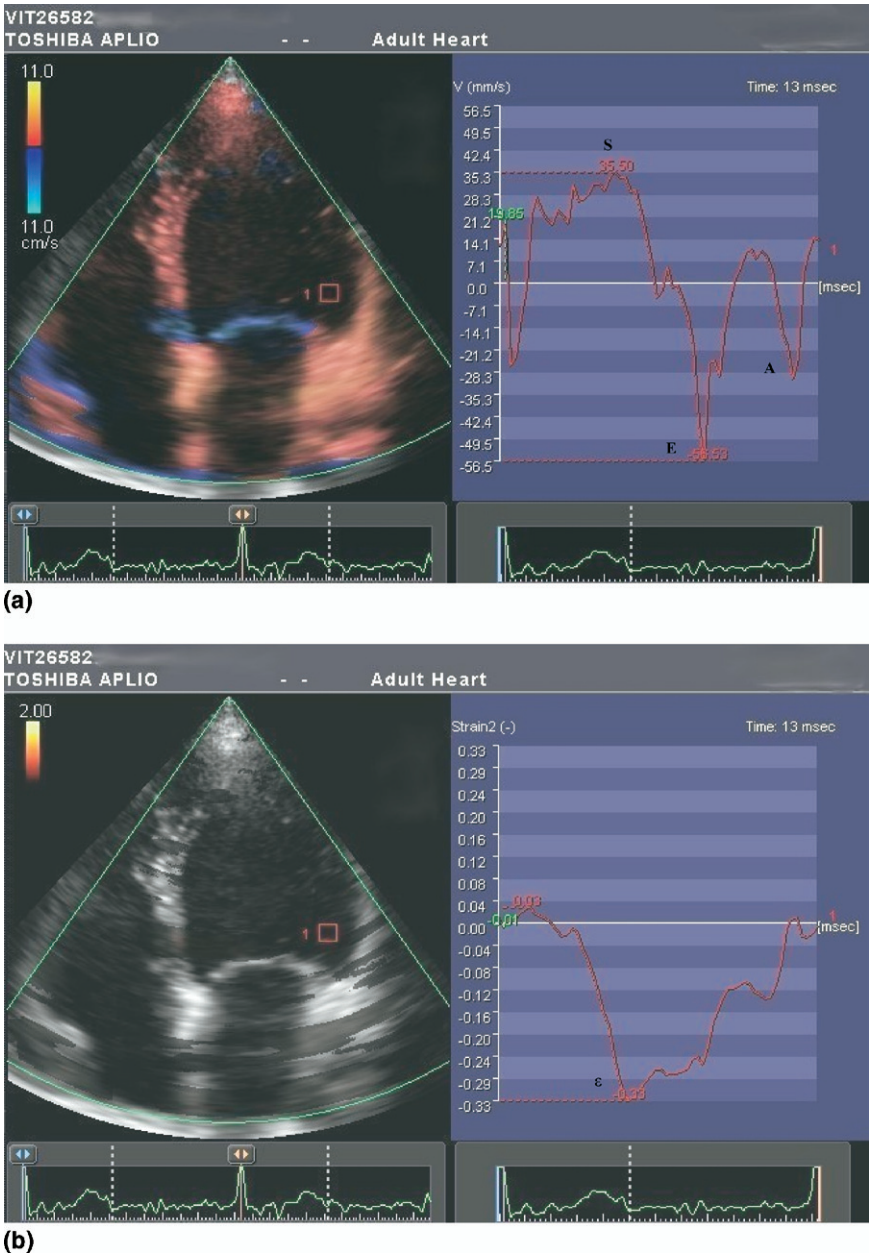

Fig. 1. Two-dimensional tissue Doppler image with sample sites at endocardial level in the basal lateral LV wall (apical four-chamber view). (A) Velocities profiles: the systolic, early diastolic and atrial induced velocities are shown. (B) Strain profiles. (C) Strain rate profiles: isovolumic contraction, systolic, isovolumic relaxation, early diastolic and atrial induced strain rate waves are shown. (D) Cyclic variation profiles. (A = late diastole; E = early diastole; IVC = isovolumic contraction; IVR = isovolumic relaxation; S = systole; ϵ = peak systolic strain.)

The main echocardiographic features in the control and aortic stenosis groups are compared in Tables 1 and 2.

2D/Doppler data

Left ventricular mass index was increased compared with normals (Table 1). Early diastolic mitral inflow velocity to atrial velocity ratio was slightly diminished and isovolumic relaxation time was slightly increased compared with controls. End-systolic left ventricular meridional wall stress (ESS_m) and circumferential wall stress (ESS_c) were slightly increased compared with normal subjects. Although not statistically significant, there was a trend toward a higher incidence of lower LVEF and greater left atrial size in patients compared with controls. Five patients (7%) had a LVEF $<50\%$.

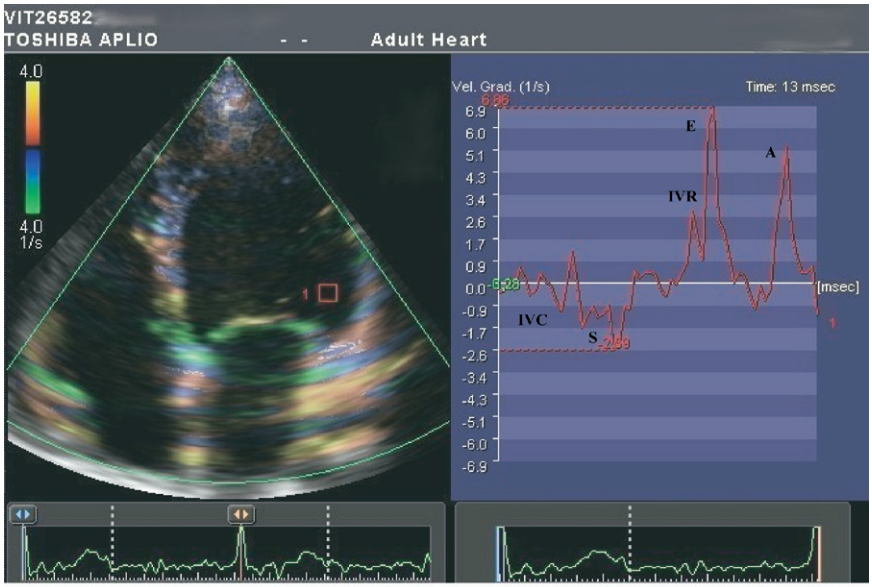

(c)

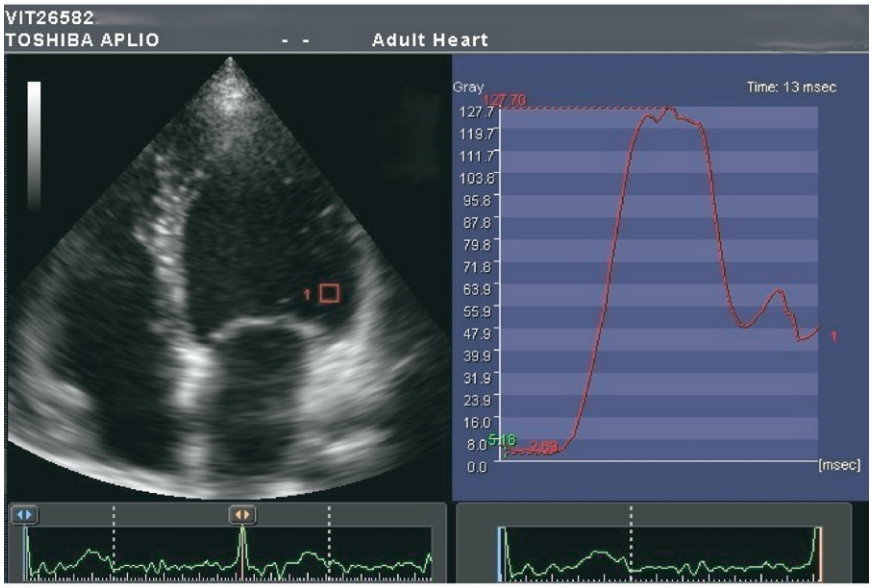

(d)

Fig. 1. *Continued.*

TDI/SRI and IB data

TDI velocity measurements of the myocardial layers showed no statistically significant difference among velocities in both pts groups although there was a trend for End velocities to be higher than those of Epi. There was a significant difference between the myocardial layers in peak systolic strain (End-ϵ 19.8 $\pm$ 7.7%, Epi-ϵ 12.7 $\pm$ 5.7%). A significant difference between the myocardial layers was shown in strain rate during systole, early diastole, isovolumic contraction and relaxation (End-SR $-2.8 \pm 1.7\ s^{-1}$, Epi-SR $-0.9 \pm 0.4\ s^{-1}$ during systole; End-SR $2.7 \pm 1.7\ s^{-1}$, Epi-SR $0.9 \pm 0.2\ s^{-1}$ during early diastole; End-SR $-1.6 \pm 1.2\ s^{-1}$, Epi-SR $-0.9 \pm 0.3\ s^{-1}$ during IC; End-SR $1.7 \pm 1.5\ s^{-1}$, Epi-SR $0.7 \pm 0.3\ s^{-1}$ during IR). A significant difference between the myocardial layers was found in cyclic variation of IB (End-CV 7.7 $\pm$ 2.3 dB, Epi-CV 6.6 $\pm$ 2.4 dB). Early diastolic endocardial strain rate (Fig. 2) showed the best correlation with transvalvar peak pressure gradients ($r = 0.76$, $p < 0.005$) and aortic valve areas ($r = 0.83$, $p < 0.001$). Compared with group 1 (Table 2, Fig. 3), group two pts showed a more marked

Table 1. 2D and Doppler echocardiographic parameters

	Controls (n = 46)	Patients (n = 68)	*p* value
Age	34.1 ± 15	31.9 ± 12	NS
Men/women, n (%)	22/14 (63)	34/23 (67)	
Heart rate, beats/min	71 ± 7	73 ± 9	NS
BSA, m^2	1.72 ± 0.26	1.75 ± 0.21	NS
LV and LA geometry			
Septal thickness, mm	10 ± 0.8	16 ± 0.6	<0.01
Posterior wall thickness, mm	10 ± 0.2	15 ± 0.12	<0.05
Wall thickness: mid-wall radius ratio	0.39 ± 0.05	0.48 ± 0.08	<0.01
LV mass, g	175 ± 24	294 ± 28	<0.05
LV mass index, g/m^2	103 ± 16	165 ± 19	<0.01
ESS_c, g/cm^2	99 ± 11	133 ± 7	<0.05
ESS_m, g/cm^2	57 ± 9	72 ± 8	<0.05
LA dimension	37 ± 5	43 ± 7	NS
LV systolic function			
LV ejection fraction, %	62 ± 7	52 ± 2	NS
LV longitudinal axis shortening, %	28 ± 14	18 ± 13	<0.01
LV mid-wall radius shortening, %	22 ± 6	21 ± 9	NS
LV internal radius shortening, %	45 ± 6	42 ± 7	NS
Cardiac output, l/min	5.8 ± 1.8	4.9 ± 1.5	NS
Cardiac index, $l/min/m^2$	3.5 ± 0.8	2.9 ± 0.7	NS
LV diastolic function			
Peak E velocity, cm/s	83 ± 8.2	79 ± 17	NS
Peak A velocity, cm/s	55 ± 11	68 ± 13	NS
E/A ratio	1.5 ± 0.5	1.1 ± 0.7	<0.05
IVRT, ms	71 ± 11	119 ± 13	<0.01
DT, ms	153 ± 25	195 ± 39	<0.01
SFF	0.41 ± 0.12	0.52 ± 0.17	NS

BSA = body surface area; DT = deceleration time; ESS_c = end-systolic circumferential wall stress; ESS_m = end-systolic meridional wall stress; IVRT = isovolumic relaxation time; LA = left atrium; LV = left ventricle; SFF = systolic filling fraction.

decrease in endocardial strain, strain rate and cyclic variation of IB ($p < 0.005$).

Systolic pressure gradients of asymptomatic patients were 38 ± 12 mm Hg and those of symptomatic patients were 65 ± 14 mm Hg ($p < 0.05$). In 32 patients, in whom cardiac catheterisation was performed, a significant correlation was shown between early diastolic endocardial strain rate and aortic peak pressure gradients ($r = 0.74$, $p < 0.005$). Aortic valve areas determined using continuity equation were significantly related to those determined using TEE planimetry ($r = 0.89$, $p < 0.001$).

In the multiple correlation analysis, factors associated with the presence of symptoms were mass index ($p < 0.05$), pressure gradient ($p < 0.01$), early diastolic wall velocity ($p < 0.05$), early diastolic annulus velocity ($p < 0.05$), peak systolic strain ($p < 0.01$), continuity aortic valve area ($p < 0.005$), TEE aortic valve area ($p < 0.005$), systolic strain rate ($p < 0.005$), early diastolic strain rate ($p < 0.001$) and cyclic variation ($p < 0.001$).

On the basis of aortic valve area (continuity), 24 patients had mild aortic stenosis (aortic valve area between 1.2 and 1.8 cm^2), 23 patients had moderate aortic stenosis (aortic valve area between 0.8 and 1.2 cm^2) and 21 patients had severe aortic stenosis (aortic valve area <0.8 cm^2). LV mass, LVEF, and SRI/IB data in asymptomatic and symptomatic patients with mild, moderate and severe aortic stenosis are reported in Table 3.

ROC curves shown in Fig. 4 suggest that the thresholds offering an adequate compromise between sensitivity and specificity for the prediction of symptoms were $\geq$60 mm Hg for the pressure gradient, ≤ 0.60 cm^2/m^2 for aortic valve area, $\leq$20% for peak systolic strain, ≤ 2.0 s^{-1} for early diastolic strain rate and $\leq$3.0 dB for cyclic variation. The area under the ROC curve (AUC), which reflects the overall performance for the prediction of symptoms, was 0.69 for the pressure gradient, 0.73 for strain, 0.76 for aortic valve area, 0.77 for cyclic variation and 0.81 for strain rate. If pressure gradient was combined with SRI/IB parameters, the AUC was significantly improved to 0.86 ($p < 0.001$). If both pressure gradient and aortic valve area were combined with SRI/IB parameters, the AUC was significantly improved to 0.89 ($p < 0.001$ compared with pressure gradient, $p < 0.005$ compared with valve area).

Data after surgery

The results of the echocardiographic studies performed 6 months after the surgical procedure (27 patients) are reported in Table 4. There was a significant reduction of LV mass index at a varying degree and a trend toward an improvement of LV ejection fraction. A parallel increase of systo-diastolic SRI parameters and cyclic variation values was obtained with higher significance.

DISCUSSION

The major result of this study is that in aortic stenosis the addition of indexes of subendocardial dysfunction such as strain, strain rate and cyclic variation of integrated backscatter to the conventional hemodynamic parameters of severity resulted in a better relationship to the symptomatic status.

Aortic stenosis and subendocardial dysfunction

Subendocardial underperfusion in aortic stenosis can be explained by several mechanisms such as increased extravascular compressive forces, inadequate capillary density in relation to the increased myocardial mass, abnormal intramyocardial small coronary arteries with luminal narrowing of small vessels caused by intimal hyperplasia and medial hypertrophy and elevation in

Table 2. TDI/SRI and IB echocardiographic parameters

	Controls (n = 46)	All pts (n = 68)	Asym. pts (n = 37)	Symp. pts (n = 31)	P1	P2	P3
S_w velocity*, cm/sec	9.4 ± 1.8	5.9 ± 1.7	7.7 ± 1.8	5.3 ± 1.3	<0.05	NS	<0.01
E_w velocity*, cm/sec	−15.3 ± 1.3	−9.6 ± 2.7	−11.4 ± 2.1	−7.8 ± 1.6	<0.05	<0.05	<0.01
A_w velocity*, cm/sec	−2.6 ± 1.7	−2.2 ± 1.4	−2.3 ± 1.1	−2.3 ± 0.6	NS	NS	NS
S_a velocity, cm/sec	8.5 ± 1.8	6.2 ± 1.5	6.7 ± 1.2	6.1 ± 0.8	<0.05	NS	<0.05
E_a velocity, cm/sec	−10.7 ± 1.4	−6.4 ± 1.5	−7.5 ± 1.2	−5.9 ± 1.4	<0.05	NS	<0.01
A_a velocity, cm/sec	−2.5 ± 1.6	−2.2 ± 1.5	−2.1 ± 1.3	−2.2 ± 0.6	NS	NS	NS
Peak S_w strain*, %	32.1 ± 10.1	19.8 ± 7.7	24.9 ± 7.2	16.7 ± 4.8	<0.005	<0.05	<0.001
IVC wall SR*, sec^{-1}	−2.7 ± 1.9	−1.6 ± 1.4	−2.1 ± 1.3	−1.4 ± 0.8	<0.001	NS	<0.001
S_w SR*, sec^{-1}	−4.8 ± 1.4	−2.8 ± 1.7	−3.6 ± 1.4	−2.4 ± 0.6	<0.005	NS	<0.005
IVR wall SR*, sec^{-1}	2.5 ± 1.3	1.7 ± 1.5	1.9 ± 1.3	1.4 ± 0.9	<0.001	<0.05	<0.001
E_w SR*, sec^{-1}	8.2 ± 1.6	2.7 ± 1.7	4.1 ± 0.5	2.1 ± 0.6	<0.001	<0.01	<0.0005
A_w SR*, sec^{-1}	2.6 ± 1.5	2.2 ± 1.4	2.3 ± 0.9	2.1 ± 1.1	NS	NS	NS
Cyclic variation*, dB	9.3 ± 2.8	7.7 ± 2.3	8.0 ± 2.1	4.6 ± 2.9	<0.001	<0.05	<0.001

A_a = mitral annular late diastolic (atrial-induced); A_w = LV wall late diastolic; E_a = mitral annular early diastolic; E_w = LV wall early diastolic; IVC = isovolumic contraction; IVR = isovolumic relaxation; S_a = mitral annular systolic; S_w = LV wall systolic.
P1: all patients (pts) compared with controls.
P2: asymptomatic patients (asym. pts) compared with controls.
P3: symptomatic patients (symp. pts) compared with controls.
* = at endocardial site.

left ventricular filling pressures (Rajappan et al. 2003). Interstitial and perivascular fibrosis and subendocardial myocytes vacuolization, necrosis or fibrosis have been described in patients with aortic stenosis and normal ejection fraction but elevated left ventricular end-diastolic pressure. With continued ischemia, eventually there is myocardial necrosis and fibrous tissue replacement, greatest in the subendocardial myocardium. The mechanism of progression from well-compensated hypertrophy to heart failure is complex. Thus, the severity of aortic stenosis and the onset of symptoms may be related not only to hemodynamic parameters as pressure gradient and aortic valve area but also to other factors linked with LV geometry and function and the status of peripheral circulation (Orsinelli et al. 1993; Omran et al. 1996; Baumgartner et al. 1999; Rajappan et al. 2003).

Excessive concentric LV hypertrophy, as defined by a relative wall thickness ratio >0.66, has been shown to be associated with a higher incidence of symptoms and with a significantly increased risk of postoperative mortality after aortic valve replacement (Orsinelli et al. 1993). It has been reported that a large proportion of patients with pure aortic stenosis (*i.e.*, patients with AS but no CAD or systemic hypertension) have a selective decrease in LV longitudinal shortening, whereas the usual indices of LV systolic function (LV ejection fraction and LV internal radius shortening fraction) remain normal (Tongue et al. 2003). These observations are consistent with the fact that, as long as there is no afterload mismatch, the increase in wall stress is mainly in the subendocardium and that subendocardial and subepicardial myocardial fiber layers are oriented longitudinally whereas the middle layer is oriented circumferentially. This explains why parameters of LV systolic function based solely on wall displacement may remain normal despite significant damage and dysfunction within the subendocardium.

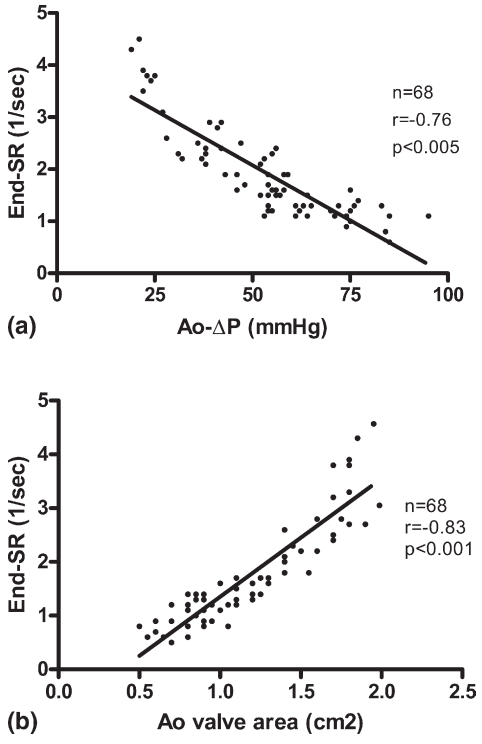

Fig. 2. Correlation between endocardial early diastolic strain rate and left ventricular outflow pressure gradient and aortic valve area in patients with aortic stenosis. (A) Left ventricular outflow pressure gradient. (B) Aortic valve area.

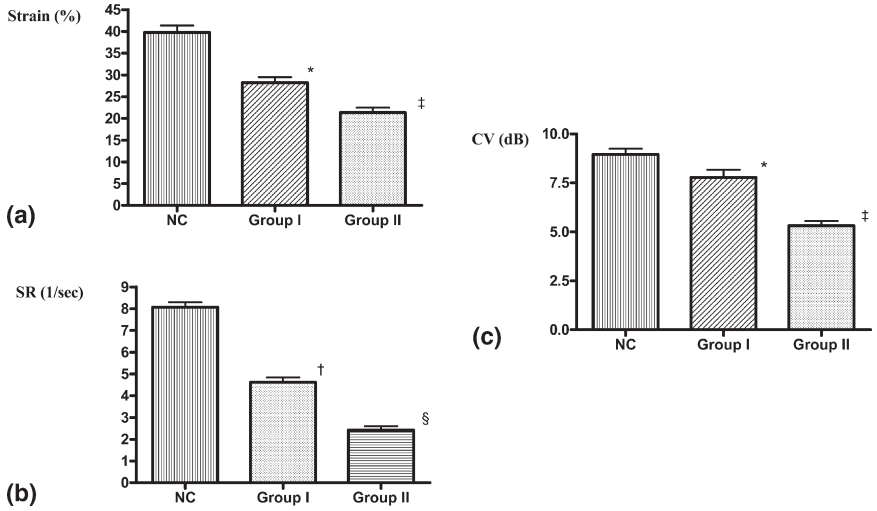

Fig. 3. Endocardial peak systolic strain, early diastolic strain rate (SR) and cyclic variation (CV) values in group 1 (asymptomatic) and group 2 (symptomatic) patients. (asterisk) $p < 0.05$ compared with normals; (dagger) $p < 0.01$ compared with normals; (double dagger) $p < 0.001$ compared with normals; (section symbol) $p < 0.0005$ compared with normals.

Subendocardial strain Doppler and integrated backscatter

Several indices provided by tissue velocity and strain techniques proved to be influenced by left ventricular pressure overload. TDI mitral annulus displacement and reduction of systolic and early diastolic peak wall velocity and its acceleration have been observed in adults (Lindstrom and Wranne 1999; Bruch et al. 2004; Bauer et al. 2004; Giorgi et al. 2005) and children (Kiraly et al. 2003; De Kort et al. 2006) with aortic stenosis. Both septal and lateral wall velocities have shown high sensitivity and specificity in detecting myocardial abnormalities (Nagueh et al. 2001; Kiraly et al. 2003). Parameters concerning the longitudinal wall movements measured in four-chamber view were more affected compared with the radial movement parameters measured in short axis view (Lindstrom and Wranne 1999; Kiraly et al. 2003) and the decrease of the systolic strain rate indices in aortic stenosis was higher and statistically more significant than that of the TDI velocity parameters. Thus, it appears that conventional echocardiography is appropriate to detect global LV dysfunction but not subclinical abnormalities, whereas new Doppler techniques can evidence regional wall dysfunction at early stages of pressure-overloaded left ventricle before ejection fraction deteriorates.

The present study was specifically designed to address to the relationship between subendocardial func-

Table 3. LV mass, LVEF and SRI/IB data in pts with mild, moderate and severe AS

	AVA 1.2-1.8 cm^2		AVA 0.8-1.2 cm^2			AVA <0.8 cm^2		
	Asymp. pts	Symp. pts	Asymp. pts	Symp. pts	*P* value	Asymp. pts	Symp. pts	*P* value
LVM (g)	195 ± 18	†	245 ± 26	329 ± 21	NS	257 ± 19	335 ± 27	NS
LVMI (g/m^2)	115 ± 12	†	137 ± 15	158 ± 18	NS	146 ± 18	182 ± 13	NS
LVEF (%)	61 ± 5	†	63 ± 6	56 ± 7	NS	60 ± 8	51 ± 6	NS
Peak systolic wall strain* (%)	26.2 ± 7.1	†	27.2 ± 9.2	19.2 ± 7.3	<0.05	25.2 ± 8.7	18.2 ± 7.6	<0.05
IVC wall SR* (sec^{-1})	−2.6 ± 1.6	†	−2.3 ± 1.8	−1.6 ± 1.3	<0.005	−2.2 ± 1.5	−1.5 ± 1.1	<0.005
Systolic wall SR* (sec^{-1})	−4.1 ± 1.4	†	−3.9 ± 1.3	−2.7 ± 1.9	NS	−3.6 ± 1.7	−2.7 ± 1.6	NS
IVR wall SR* (sec^{-1})	2.6 ± 1.1	†	2.1 ± 1.2	1.6 ± 1.2	<0.005	2.1 ± 1.1	1.4 ± 0.9	<0.005
Early diastolic wall SR* (sec^{-1})	4.7 ± 0.6	†	4.2 ± 0.9	2.5 ± 0.5	<0.005	4.3 ± 1.1	2.3 ± 0.8	<0.001
Late diastolic wall SR* (sec^{-1})	2.5 ± 1.5	†	2.4 ± 1.3	2.2 ± 1.5	NS	2.5 ± 1.1	2.1 ± 1.7	NS
Cyclic variation* (dB)	8.9 ± 2.8	†	8.7 ± 2.5	6.1 ± 2.1	<0.05	8.1 ± 1.9	4.7 ± 2.2	<0.05

Asymp. pts = asymptomatic patients; AVA = aortic valve area; IVC = isovolumic contraction; IVR = isovolumic relaxation; LV = left ventricle; LVEF = left ventricular ejection fraction; LVM = left ventricular mass; LVMI = left ventricular mass index; SR = strain rate; Symp. pts = symptomatic patients; * = at endocardial site; † = too few symptomatic patients to perform statistical analysis.

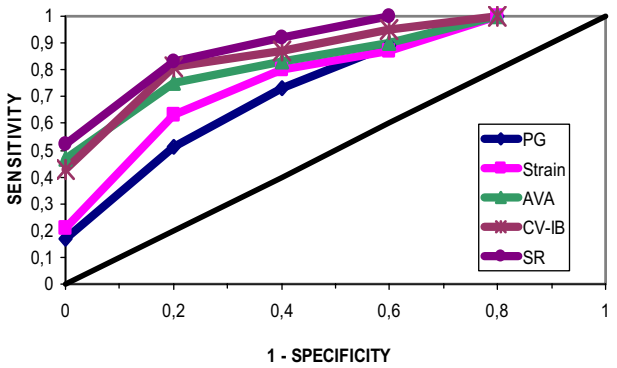

Fig. 4. Comparison between the area under the curve (AUC) of the receiver-operating characteristic curves obtained for the echocardiographic variables analysed: pressure gradient (AUC 0.69), peak systolic strain (AUC 0.73), aortic valve area (AUC 0.76), cyclic variation of IB (AUC 0.77) and early diastolic strain rate (AUC 0.81). By combining pressure gradient and aortic valve area with SRI/IB parameters, the AUC was significantly improved to 0.89 ($p < 0.001$ compared with pressure gradient, $p < 0.005$ compared with valve area). The variables more predictive of symptoms are those with the highest AUC.

tion and symptomatic status in patients with aortic stenosis. Our results show that quantitative assessment of subendocardial dysfunction gives additional information in asymptomatic patients and helps in the judgment of severity if compared with standard indexes such as high pressure gradient, reduced aortic valve area and increased LV mass. Early diastolic endocardial strain rate showed the best correlation with pressure gradients and valve areas and symptomatic patients showed a more marked decrease in endocardial strain and strain rate. The more significant decrease of the strain rate parameters compared with velocity parameters suggests the intrinsically higher accuracy of strain rate measurement (Hashimoto et al. 2003; Matre et al. 2005) due to neutralisation of the influence of the global heart movement.

It is known (Borow et al. 1985; Mirsky et al. 1988) that for any level of contractility, the end-systolic fiber length is linearly related to the end-systolic force (*i.e.*, wall stress). In our study, both meridional and circumferential stresses were used to quantitate afterload. Although hypertrophy in patients with AS results in normalization of peak systolic wall stress so that the maximum force per unit cross-sectional area is not elevated, there is myocardial deterioration in the very late stages of this disease. This explains the highest values we found in patients with AS compared with normal controls (Table 1) but also the less discriminating power in differentiating patients from normal controls compared with strain parameters (Table 2) and lack of correlation with symptomatic status. Since what gives rise to the total muscle load during ejection is the dynamic interplay of the total ventricular pressure load with complex geometric and histoarchitectonic factors in various adaptations of the "law of Laplace", a strain-stress evaluation can give insight into left ventricular mechanics in terms of force-shortening-velocity characteristics.

New endocardial measures could be related to symptomatic state merely because they are a reflection of greater left ventricular hypertrophy and/or LV pressure overload. However, SRI/IB parameters had a higher discriminating power than LV wall thickness and mass in differentiating patients with aortic stenosis from normal controls (Tables 1 and 2). Furthermore, after selecting patients with the same hemodynamic severity (Table 3), a significant difference in SRI/IB parameters was found between patients with and those without symptoms whereas no significant difference in LV mass index or ejection fraction was observed. This is particularly relevant in those patients judged to be of intermediate severity on the basis of aortic valve area. On the other hand, previous reports have shown tissue Doppler velocities changes in patients with LV pressure overload before and independently of hypertrophy (Nagueh et al. 2001; Vinereanu et al. 2001). Thus, the decrease of early diastolic peak wall velocity and strain rate might reflect a reduced relaxation rate of the stiffer left ventricular myocardium in patients with aortic stenosis.

Cyclic variation of integrated backscatter is also of great potential interest as a marker of myocardial ischemia and/or fibrosis. The possibility to assess the cyclic variation in the different myocardial layers allows the assessment of contractility gradients across the myocardial wall and may help to identify minor degrees of myocardial dysfunction, which are unable to impair the

Table 4. Two-dimensional and SRI/IB values before and after surgery (27 pts)

	Before surgery	After surgery	*p*-value
LV ejection fraction	47 ± 13	53 ± 14	NS
LV mass index	184 ± 14	129 ± 11	<0.01
S_w velocity*, cm/sec	5.3 ± 1.6	8.8 ± 1.2	<0.01
E_w velocity*, cm/sec	−9.2 ± 2.2	−14.3 ± 1.4	<0.01
A_w velocity*, cm/sec	−2.3 ± 1.5	−2.8 ± 1.8	NS
S_a velocity, cm/sec	5.2 ± 1.3	8.4 ± 1.3	<0.01
E_a velocity, cm/sec	−5.4 ± 1.2	−9.1 ± 1.5	<0.01
A_a velocity, cm/sec	−2.2 ± 1.7	−2.6 ± 1.5	NS
Peak systolic wall strain*, %	15.8 ± 5.7	29.2 ± 8.1	<0.005
IVC wall strain rate*, sec^{-1}	−1.7 ± 1.4	−2.8 ± 1.9	<0.001
Systolic wall strain rate*, sec^{-1}	−2.7 ± 1.6	−4.7 ± 1.5	<0.005
IVR wall strain rate*, sec^{-1}	1.5 ± 1.1	2.4 ± 1.6	<0.001
Early diastolic wall strain rate*, sec^{-1}	2.8 ± 1.5	7.7 ± 1.7	<0.001
Late diastolic wall strain rate*, sec^{-1}	2.2 ± 1.4	2.6 ± 1.9	NS
Cyclic variation*, dB	4.8 ± 2.2	9.4 ± 2.3	<0.001

Abbreviations as in Table 2.

transmural wall function and thereby do not modify the regional wall thickening.

It cannot be excluded that subendocardial ischemia due to coexisting conditions such as coronary artery disease (CAD) or hypertension can also contribute to the decrease of strain parameters. However, our population consisted predominantly of young adults with congenital stenosis with no incidence of obstructive coronary artery disease. Although aortic valve stenosis has been considered to most commonly be the result of degenerative process, recent data suggest that an underlying congenitally malformed valve is more common than a tricuspid aortic valve (Roberts and Ko 2005). Nonetheless, in older patients with aortic stenosis, LV longitudinal shortening measured with other methods remained as an independent predictor of symptoms even when CAD or hypertension were taken into account in the multivariate analysis (Tongue et al. 2003).

Aortic surgery, reducing the pressure overload caused by aortic stenosis, stimulates a normalization of LV hemodynamics with improvement of subendocardial function and SRI/IB parameters to a greater extent compared with LV mass.

Clinical implications

Valvular aortic stenosis should be considered as a dynamic lesion. Progressive thickening and obstruction of a bicuspid or trileaflet aortic valve is due to an active disease process and promotes progressive LV pressure overload. A simple, reliable method to detect subendocardial dysfunction in the setting of myocardial hypertrophy could provide an early warning sign to identify asymptomatic patients at high risk. The management of patients with aortic stenosis is challenging and the aim of the follow-up is to assess the medical interventions that might slow or prevent disease progression as well as to determine the optimal timing for surgery. Exercise testing appears to be useful in asymptomatic patients (Lancellotti et al. 2005) but exertional hypotension may lead to serious complications even with "asymptomatic" aortic stenosis. The results of the present study suggest that strain Doppler and integrated backscatter echocardiography may aid in the assessment of the severity of disease showing subendocardial damage. On this basis, patients with peak systolic strain $\leq$20%, early diastolic strain rate $\leq$2.0 s^{-1} and cyclic variation $\leq$3.0 dB are classified as having severe aortic stenosis. This can be especially valuable in patients that are judged at an intermediate stage by conventional grading of severity and constitute a gray zone into which some cases of critical stenosis may fall. Since strain/backscatter parameters were decreased in symptomatic as well in asymptomatic patients compared with normals, they can be an effective tool in identifying asymptomatic patients with subendocardial dysfunction (who require "prophylactic" valve replacement).

Limitations of the study

Strain measurements are angle dependent, as other Doppler modalities. Interpretations of strains should be performed with caution if tissue direction deviates more than 30 degrees from the beam direction. Since angle problem is a significant limitation of this technique, repositioning of the transducer may help to avoid the problem. However, despite its angle dependence, echocardiographic SR measurement is superior to magnetic resonance imaging with respect to spatial and temporal resolution (Yeon et al. 2001).

Strain profiles and curves do not always return to zero baseline at end diastole. This may be in part due to the mathematical integration algorithm but may also be caused by the fact that the wall itself does not return to exactly the same state of deformation at the end of the cycle as was the case at the start. This aspect could be related to several factors, including the normal beat-to-beat variation in stroke volume.

SR profiles tend to be more noisy than TDI data and SR amplitude is a measurement with problems of reproducibility. However, it has been reported (Greenberg et al. 2002) that amplitudes of SR have close relationships with maximal dP/dt derived from LV pressure and reflect LV contractility as long as regional wall motion is intact. Moreover, the application of automatic sample volume tissue tracking techniques aid continuous sampling of the moving walls and improve the quality of the traces.

Echocardiographic backscatter is influenced by native ultrasound signal modifications as a result of manifold electronic processing and mainly by the type of gray level preprocessing map. In addition, such analysis requires an excellent acoustic window to be feasible and can better assess cyclic variation echodensity changes in approaches in which the ultrasonic beams impact perpendicularly to the fibre orientation. In the apical views, the peak and nadir of the cyclic IB are often at a different phase of the cardiac cycle compared with the parasternal views as a result of the orientation of the myocardial elements relative to the angle of insonation (anisotropic effect). However, significant differences between normal and ischemic or fibrotic myocardial territories have been reported for both views (Finch-Johnston et al. 2000; Hancock et al. 2004).

The selection of our study population (patients aged 15- to 52-y-old) makes this sample not representative of the average patient encountered in a standard cardiology practice. The average aortic stenosis patient tends to be older and with degenerative changes of the aortic valve leaflets as opposed to younger and with congenital bi-

cuspid valve (Roberts and Ko 2005). We have chosen this population to avoid the confounding factors associated with hypertension and coronary artery disease but these results cannot be extrapolated to a general group of patients with larger comorbidity.

Finally, the enrolment of a larger number of patients and a longer follow-up would be desirable to confirm our observations showing more severe abnormalities of the ultrasound parameters in symptomatic patients and to prove that asymptomatic patients with abnormal ultrasound parameters are more likely to become symptomatic.

CONCLUSION

Despite some limitations, our results indicate that a reduction of strain, strain rate and cyclic variation values may be a sensitive marker of subendocardial myocardial dysfunction and improve the detection of high risk patients with aortic stenosis. A systematic assessment of these parameters might be complementary to the evaluation of pressure gradient and indexed aortic valve area in judging the severity of this disease.

Acknowledgments—This work was supported by a research grant by the Italian Ministry of Research. The authors thank Manuela Antonucci and Sara Dolfini for their assistance in the preparation of the manuscript.

REFERENCES

Appleton CP, Galloway JM, Gonzalez MS, et al. Estimation of left ventricular filling pressures using two-dimensional and Doppler echocardiography in adult cardiac patients. Additional value of analysing left atrial size, left atrial ejection fraction and the difference in the duration of pulmonary venous and mitral flow velocities at atrial contraction. J Am Coll Cardiol 1993;22:1972–1982.

Bauer F, Eltchaninoff H, Tron C, et al. Acute improvement in global and regional left ventricular systolic function after percutaneous heart valve implantation in patients with symptomatic aortic stenosis. Circulation 2004;110:1473–1476.

Baumgartner H, Stefenelli T, Niederberger J, et al. Overestimation of catheter gradients by Doppler ultrasound in patients with aortic stenosis: A predictable manifestation of pressure recovery. J Am Coll Cardiol 1999;33:1655–1661.

Bonow RO, Carabello BA, de Leon AC, Jr., et al. Guidelines for the managements of patients with valvular heart disease. Executive summary. A report of the American College of Cardiology/American Heart association task force on practice guidelines (Committee on management of patients with valvular heart disease). Circulation 1998;98:1949–1984.

Borow KM, Colan SD, Neumann A. Altered left ventricular mechanics in patients with valvular aortic stenosis and coarctation of the aorta: Effects on systolic performance and late outcome. Circulation 1985;72:515–522.

Bruch C, Stypmann J, Grude M, et al. Tissue Doppler imaging in patients with moderate to severe aortic valve stenosis: Clinical usefulness and diagnostic accuracy. Am Heart J 2004;148:696–702.

De Kort E, Thijssen JM, Daniels O, de Korte CL, Kapusta L. Improvement of heart function after balloon dilation of congenital valvar aortic stenosis: A pilot study with ultrasound tissue Doppler and strain rate imaging. Ultrasound Med Biol 2006;32:1123–1128.

Devereux RB, Alonso DR, Lutas EM, et al. Echocardiographic assessment of left ventricular hypertrophy: Comparison to necropsy findings. Am J Cardiol 1986;57:450–458.

Di Bello V, Giorgi D, Viacava P, et al. Severe aortic stenosis and myocardial function. Diagnostic and prognostic usefulness of ultrasonic integrated backscatter analysis. Circulation 2004;110:849–855.

Donal E, Novaro GM, Deserrano D, et al. Planimetric assessment of anatomic valve area overestimates effective orifice area in bicuspid aortic stenosis. J Am Soc Echocardiogr 2005;18:1392–1398.

Finch-Johnston AE, Gussak HM, Mobley J, et al. Cyclic variation of integrated backscatter: Dependence of time delay on the echocardiographic view used and the myocardial segment analysed. J Am Soc Echocardiogr 2000;13:9–17.

Garcia D, Pibarot P, Dumesnil JG, et al. Assessment of aortic valve stenosis severity: A new index based on the energy loss concept. Circulation 2000;101:765–771.

Giorgi D, Di Bello V, Talini E, et al. Myocardial function in severe aortic stenosis before and after aortic valve replacement: A Doppler tissue imaging study. J Am Soc Echocardiogr 2005;18:8–14.

Greenberg NL, Firstenberg MS, Castro PL, et al. Doppler-derived myocardial systolic strain rate is a strong index of left ventricular contractility. Circulation 2002;105:99–105.

Hancock JE, Cooke JC, Monaghan MJ. Effect of harmonic imaging on the measurement of ultrasonic integrated backscatter and its interpretation in patients following myocardial infarction. Eur J Echocardiography 2004;189–195.

Hashimoto I, Li X, Hejmadi Bhat A, et al. Myocardial strain rate is a superior method for evaluation of left ventricular subendocardial function compared with tissue Doppler imaging. J Am Coll Cardiol 2003;42:1574–1583.

Hoffmann R, Flachskampf FA, Hanrath P. Planimetry of orifice area in aortic stenosis using multiplane transesophageal echocardiography. J Am Coll Cardiol 1993;22:529–534.

Isaaz K, Thompson A, Ethevenot G, et al. Doppler echocardiographic measurement of low velocity motion of the left ventricular wall. Am J Cardiol 1989;64:66–75.

Kiraly P, Kapusta L, Thijssen JM, Daniels O. Left ventricular myocardial function in congenital valvar aortic stenosis assessed by ultrasound tissue-velocity and strain rate techniques. Ultrasound Med Biol 2003;29:615–620.

Kowalski M, Kukulski T, Jamla F, et al. Can natural strain and strain rate quantify regional myocardial deformation? A study in healthy subjects. Ultrasound Med Biol 2001;27:1087–1097.

Lancellotti P, Lebois F, Simon M, et al. Prognostic importance of quantitative exercise Doppler echocardiography in asymptomatic valvular aortic stenosis. Circulation 2005;112(Suppl. I):I377–1382.

Lindstrom L, Wranne B. Pulsed tissue Doppler evaluation of mitral annulus motion: A new window to assessment of diastolic function. Clin Physiol 1999;19:1–10.

Matre K, Fannelop T, Dahle GO, Heimdal A, Grong K. Radial strain gradient across the normal myocardial wall in open-chest pigs measured with Doppler strain rate imaging. J Am Soc Echocardiogr 2005;18:1066–1073.

McDicken WN, Sutherland GR, Moran CM, Gordon LN. Colour Doppler velocity imaging of the myocardium. Ultrasound Med Biol 1992;18:651–654.

Metz CE. Receiver operating characteristic methodology in radiologic imaging. Invest Radiol 1986;21:720–733.

Mirsky I, Corin WJ, Muralami T, et al. Correction for preload in assessment of myocardial contractility in aortic and mitral valve disease. Application of the concept of systolic myocardial stiffness. Circulation 1988;78:68–80.

Nagueh SF, Bachinski LL, Meyer D, et al. Tissue Doppler imaging consistently detects myocardial abnormalities in patients with hypertrophic cardiomyopathy and provides a novel means for an early diagnosis before and independently of hypertrophy. Circulation 2001;104:128–130.

Oh JK, Taliercio CP, Holmes DR Jr., et al. Prediction of the severity of aortic stenosis by Doppler aortic valve area determination: Prospec-

tive Doppler-catheterization correlation in 100 patients. J Am Coll Cardiol 1988;11:1227–1234.

Omran H, Fehske W, Rabahieh R, Hagendorff A, Luderitz B. Relation between symptoms and profiles of coronary artery blood flow velocities in patients with aortic valve stenosis: A study using transoesophageal Doppler echocardiography. Heart 1996;75: 377–383.

Orsinelli DA, Aurigemma GP, Battista S, et al. Left ventricular hypertrophy and mortality after aortic valve replacement for aortic stenosis. A high risk subgroup identified by preoperative relative wall thickness. J Am Coll Cardiol 1993;22:1679–1683.

Otto CM. Timing of aortic surgery. Heart 2000;84:211–218.

Rajappan K, Rimoldi OE, Camici PG, et al. Functional changes in coronary microcirculation after valve replacement in patients with aortic stenosis. Circulation 2003;107:3170–3175.

Rask LP, Karp KH, Eriksson NP. Flow dependence of the aortic valve area in patients with aortic stenosis: Assessment by application of the continuity equation. J Am Soc Echocardiogr 1996;9:295–299.

Roberts WC, Ko JM. Frequency by decades of unicuspid, bicuspid, and tricuspid aortic valves in adults having isolated aortic valve replacement for aortic stenosis, with or without associated aortic regurgitation. Circulation 2005;111:920–925.

Rosenhek R, Binder T, Porenta G, et al. Predictors of outcome in severe, asymptomatic aortic stenosis. N Engl J Med 2000;343: 611–617.

Schiller NB, Shah PM, Crawford M, et al. Recommendations for quantitation of the left ventricle by two-dimensional echocardiography. American Society of Echocardiography Committee on Standards, Subcommittee on Quantitation of Two Dimensional Echocardiograms. J Am Soc Echocardiogr 1989;2:358–367.

Stoylen A, Slordahl S, Skjelvan GK, et al. Strain rate imaging in normal and reduced diastolic function: Comparison with pulsed Doppler Tissue Doppler imaging of the mitral annulus. J Am Soc Echocardiogr 2001;14:264–274.

Sutherland GR, Di Salvo G, Claus P, et al. Strain and strain rate imaging: A new clinical approach to quantifying regional myocardial function. J Am Soc Echocardiogr 2004;17:788–802.

Tenenbaum A, Motro M, Hod H, et al. Shortened Doppler-derived mitral A wave deceleration time: An important predictor of elevated left ventricular filling pressure. J Am Coll Cardiol 1996;27: 700–705.

Tongue AG, Dumesnil JG, Laforest I, et al. Left ventricular longitudinal shortening in patients with aortic stenosis: Relationship with symptomatic status. J Heart Valve Dis 2003;12:142–149.

Vinereanu D, Florescu N, Sculthorpe N, et al. Differentiation between pathologic and physiologic left ventricular hypertrophy by tissue Doppler assessment of long-axis function in patients with hypertrophic cardiomyopathy or systemic hypertension and in athletes. Am J Cardiol 2001;88:53–58.

Vitarelli A, Conde Y, Ferro Luzi M, et al. Transesophageal dobutamine stress echocardiography with tissue Doppler imaging for detection and assessment of coronary artery disease. J Investig Med 2001; 49:534–543.

Vitarelli A, Conde Y, Cimino E, et al. Evaluation of subendocardial ischemia by strain Doppler echocardiography in patients with left ventricular outflow tract obstruction. Eur J Echocardiography 2003; 4(Suppl. 1):S62.

Yeon SB, Reichek N, Tallant BA, et al. Validation of *in vivo* myocardial strain measurement by magnetic resonance tagging with sonomicrometry. J Am Coll Cardiol 2001;38:555–561.